Radiation hardness of plastic scintillators for the Tile Calorimeter of the ATLAS detector

2015 J. Phys.: Conf. Ser. 623 012016

(http://iopscience.iop.org/1742-6596/623/1/012016)

Radiation hardness of plastic scintillators for the Tile Calorimeter of the ATLAS detector

H Jivan[1,2], B Mellado[1], E Sideras-Haddad[1,2], R Erasmus[1], S Liao[1], M Madhuku[3], G Peters[1], O Solvyanov[4]

1: University of the Witwatersrand, 1 Jan Smuts Avenue, Braamfontein 2000, Johannesburg.
2: DST-NRF Centre for Excellence in Strong Materials
3: iThemba LABS, North, Empire Road, Braamfontein 2000, Johannesburg.
4: European Organization for Nuclear Research (CERN), CH-1211 Genève 23, Suisse

Email: harshna.jivan@gmail.com

Abstract The radiation damage in polyvinyl toluene based plastic scintillator EJ200 obtained from ELJEN technology was investigated. This forms part of a comparative study conducted to aid in the upgrade of the Tile Calorimeter of the ATLAS detector during which the Gap scintillators will be replaced. Samples subjected to 6 MeV proton irradiation using the tandem accelerator of iThemba LABS, were irradiated with doses of approximately 0.8 MGy, 8 MGy, 25 MGy and 80 MGy. The optical properties were investigated using transmission spectroscopy whilst structural damage was assessed using Raman spectroscopy. Findings indicate that for the dose of 0.8 MGy, no structural damage occurs but a breakdown in the light transfer between base and fluor dopants is observed. For doses of 8 MGy to 80 MGy, structural damage leads to hydrogen loss in the benzene ring of the PVT base which forms free radicals. This results in an additional absorptive component causing increased transmission loss as dose is increased.

1. Introduction

The Tile Calorimeter of the ATLAS detector, is a hadronic calorimeter responsible for recording the energy and trajectory of hadrons, taus as well as jets of quarks and gluons that result from the proton-proton collisions within the Large Hadron Collider of CERN. The Tile Calorimeter consists of a central barrel and two extended barrels which each contain 64 azimuthal modules. Each module contains a matrix of steel plates with tiles of plastic scintillators sandwiched in between. The steel plates act as an absorber medium, converting the incoming jets to a 'shower' of particles whilst the scintillator tiles absorb energy from the incoming particles and fluoresce to emit light. This light is passed through wavelength shifting optical fibres and detected by photomultiplier tubes. The signal is further processed with readout electronics in order to digitize the data for analysis thereafter. In addition, the GAP region between the central and extended barrels, where many of the read-out electronics components are housed, contain additional scintillator plates. These assist with reconstruction of missing transverse energy within this region. [1]

Plastic scintillators in specific are employed within the detector due to their properties of high optical transmission and fast rise and decay times. This enables efficient data capture since fast signal pulses can be generated [2]. In addition, plastic scintillators are easier to manufacture as compared to inorganic crystals which require special growing methods, and are more cost effective [3] for covering the typically large detector areas. The main problem encountered by plastic scintillators however, is radiation damage incurred due to their interactions with the ionizing particles to be detected. This damage leads to a significant decrease in the light yield of the scintillator and introduces an error into the time-of flight data acquired.

With the LHC gearing up to run proton collisions at increased center of mass energy and higher luminosities, the radiation environment within the ATLAS detector is expected to become much harsher. The Tile Calorimeter has therefore implemented a series of upgrades in order to ensure that the detector performance can be sustained for several years to come. Part of phase two of this upgrade will be implemented in 2018 where the current crack scintillators from the GAP region of the Tile Calorimeter will be replaced with more radiation hard plastics. To aid in the choice of a replacement candidate, this comparative study is underway which examines the radiation hardness of several commercially available plastic scintillators. In addition, the study aims to further understand the type of structural damage that these plastics undergo which may assist in future developments of radiation tolerant plastic scintillators. In these proceedings, we present preliminary results for EJ200, a polyvinyl toluene based plastic obtained from ELJEN Technologies.

2. The Scintillation mechanism

Plastic scintillators primarily consist of organic fluors suspended in a polymer base. The polymer base that is employed generally contains some type of aromatic ring structure which gives rise to a delocalized π-electron structure within the molecule. When ionizing radiation impinges the scintillator, some of its kinetic energy may be absorbed by these delocalized π-electrons, resulting in molecular excitations. The absorption is typically exhibited in the visible and ultra-violet regions corresponding to excitation of the singlet π-electron state. The energy level diagram of a π-electron is shown in Figure 1 below. For transitions from the lowest vibrational first excited state to the ground state, prompt fluorescence occurs whereby energy is emitted in the form of light of a characteristic wavelength. This fluorescence process forms the basic mechanism for scintillation in organic plastic scintillators. [2]

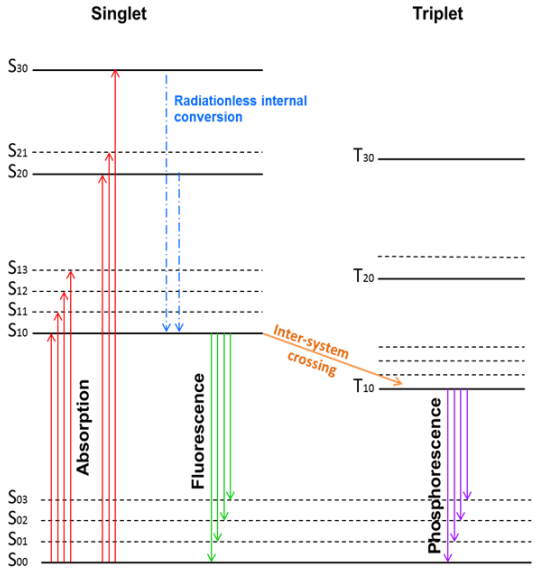

Figure 1: Energy level diagram of an organic molecule with π-electron structure, adapted from[2].The singlet states with spin 0 are labelled Sab and the triplet states of spin 1 are labelled Tab where a indicates the excitation level and b indicates the vibrational state of that level.

The energy of the fluorescent light is generally less than the energy required for absorption, however a small overlap between the absorption and emission spectra may occur. In order to prevent self-absorption of scintillation light, small concentrations of primary fluors are added to the plastic polymer. These ensure that the plastic scintillator is transparent to its own scintillation light. Occasionally, a secondary fluor may be added which acts specifically as a wavelength shifter. This is used in order to ensure that the wavelength of light leaving the scintillator is suitable for detection by optical fibres which lead to photomultiplier tubes. [4]

Plastic scintillator EJ200 is composed of a polyvinyl toluene base and 3% of added organic fluors. Polyvinyl toluene consists of long chains of vinyl toluene molecules that encompass a benzene ring (C_6H_4) bonded to a methyl group (CH_3) and a vinyl group (CH_2-CH-). Information on the exact composition of the doped fluors are not made public by the manufacturers. Some important properties of EJ200 are listed in table 1 below.

Table 1: Properties of plastic scintillator EJ200 as provided by the manufacturers [5]

	EJ200
Light Output (% Anthracene)	64
Wavelength of maximum emission (nm)	425
Rise time (ns)	0.9
Decay time (ns)	2.1
Refractive index	1.58

3. Experimental Procedure

The tandem accelerator of iThemba LABS in Gauteng was used to irradiate samples with 6 MeV protons. To ensure that the study simulated a similar type of particle-scintillator interaction as observed in the Tile Calorimeter, protons would be required to pass through the samples whilst imparting energy primarily through ionization losses. In order to ensure this, SRIM simulations were performed to determine the stopping range of 6 MeV protons within the plastic material. Based on these simulations, several samples were cut and polished to dimensions of 0.5 cm by 0.5 cm, with thickness of ~350 μm. A polishing procedure based on standard metallographic techniques was employed. Thereafter, samples were irradiated to doses of 0.8 MGy, 8 MGy, 25 MGy and 80 MGy. Quadrupole magnets were used to focus the proton beam to a spot size of ~20-30 μm and the beam was then scanned in the x and y plane to achieve an irradiated area of approximately 1.8 mm by 1.8 mm.

The effects of proton damage on the optical properties of the samples were characterized by conducting light transmission experiments. Transmission spectroscopy was conducted using the Varian Carry 500 spectrophotometer. Light transmission was measured relative to transmission in air over a range of 200-800 nm. Transmission spectra were collected prior to irradiation as well as over several days after.

The structural damage undergone by the scintillators were then investigated using Raman spectroscopy. Raman spectra were obtained for the un-irradiated control samples as well as on the 0.8 MGy and 8 MGy irradiated samples using the Horiba Jobin-Yvon Raman spectrograph. An Argon laser was used to provide a 515 nm excitation wavelength. Raman studies were conducted 3 days, 10 days and 4 weeks after irradiation.

In addition, light yield studies on the proton damaged samples are to be carried out whereby the scintillator's response to 0.5 MeV gamma rays emitted by a ^{90}Sr source will be measured using the light box set-up at CERN. In these experiments, the sample will be coupled to two Kuraray Y-11(200) optical fibers which will be connected to a standard Tile Calorimeter photomultiplier tube. As light yield experiments are to be conducted several weeks after irradiation, this will provide time for partial recovery in the scintillators.

4. Light Transmission Results and Analysis

The ratio of transmission in each irradiated EJ200 sample relative to its transmission before irradiation for several doses as a function of wavelength is shown in Figure 2 below. Absorption in the PVT base occurs over 240 nm to 300 nm whilst absorption in the fluors is expected to occur over 270 nm to 400 nm. For the dose of 0.8 MGy, a transmission dip at lower wavelengths is observed, followed by a peak over 320-400 nm. This feature indicates that a competitive absorptive process has developed between the primary and secondary fluors.

As the dose increases, we observe the formation of an absorptive tint whereby the absorption drop-off shifts to higher wavelengths. This implies that additional absorbing species such as free radicals are forming within the scintillator and leads to a further decrease in light emitted by the scintillator. This additional absorption component may also reduce the attenuation length of the scintillation light as described by C. Zorn (1993) [6].

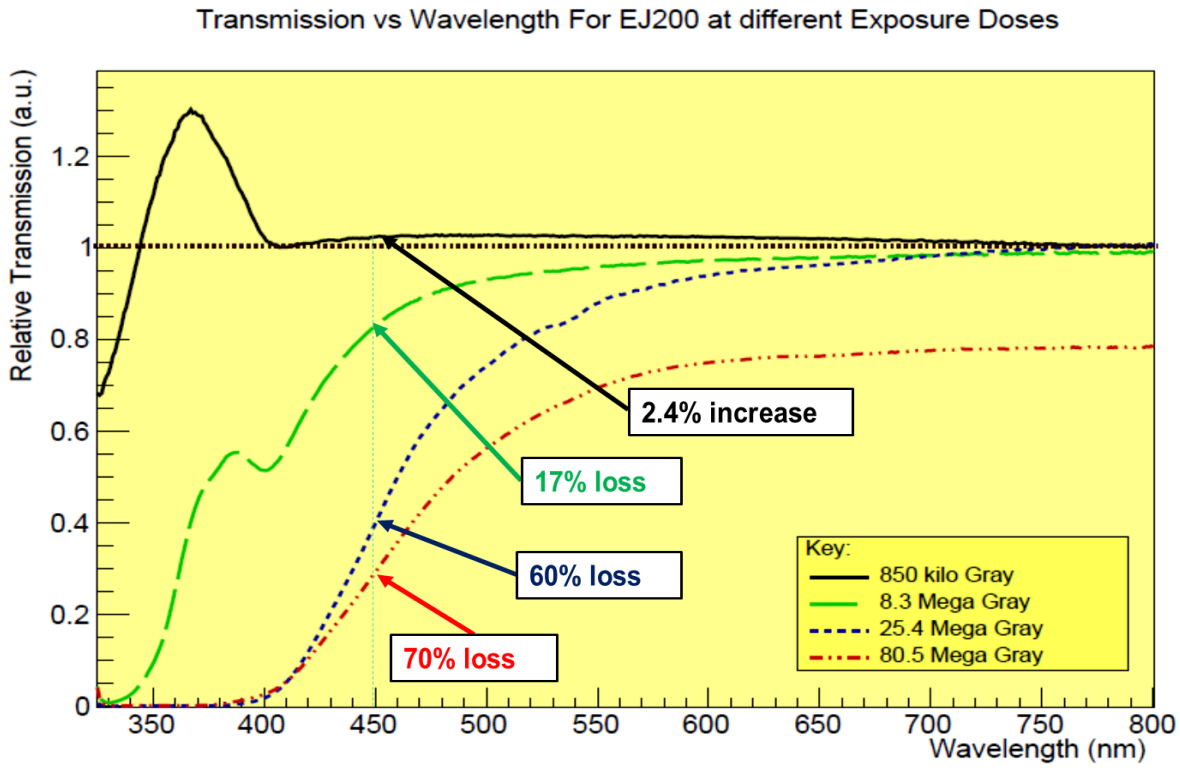

Figure 2: Ratio of transmission in irradiated sample to transmission before irradiation for EJ200 samples irradiated over several doses.

5. Raman Spectroscopy Results and Analysis

Raman spectra were obtained for the 0.8 MGy samples, 8 MGy samples as well as for un-irradiated control samples. The samples irradiated to 0.8 MGy maintained their structure and very little damage was observed. In the 8 MGy sample, an increased amount of background fluorescence could be observed which may be due to free radicals interacting with the excitation light. Raman spectroscopy could not be performed for the high dose of 80 MGy because this background fluorescence becomes too large to obtain an experimentally viable spectrum. Figure 3 shows the background subtracted Raman spectrum for the 8 MGy irradiated sample taken over several days.

The peaks observed are allocated to the characteristic functional groups or vibrational groups using the Raman Peak assignment datasheet from Horiba Jobin-Yvon. The peak assignment is summarized in Table 2. An additional peak (X) was found to form after irradiation but disappeared over time as the scintillator healed. In order to gauge changes in the amount of specific species present, the intensities of the various peaks were plotted relative to peak 13 which represents the C-C bond typically found in benzene rings. This plot is shown in Figure 4.

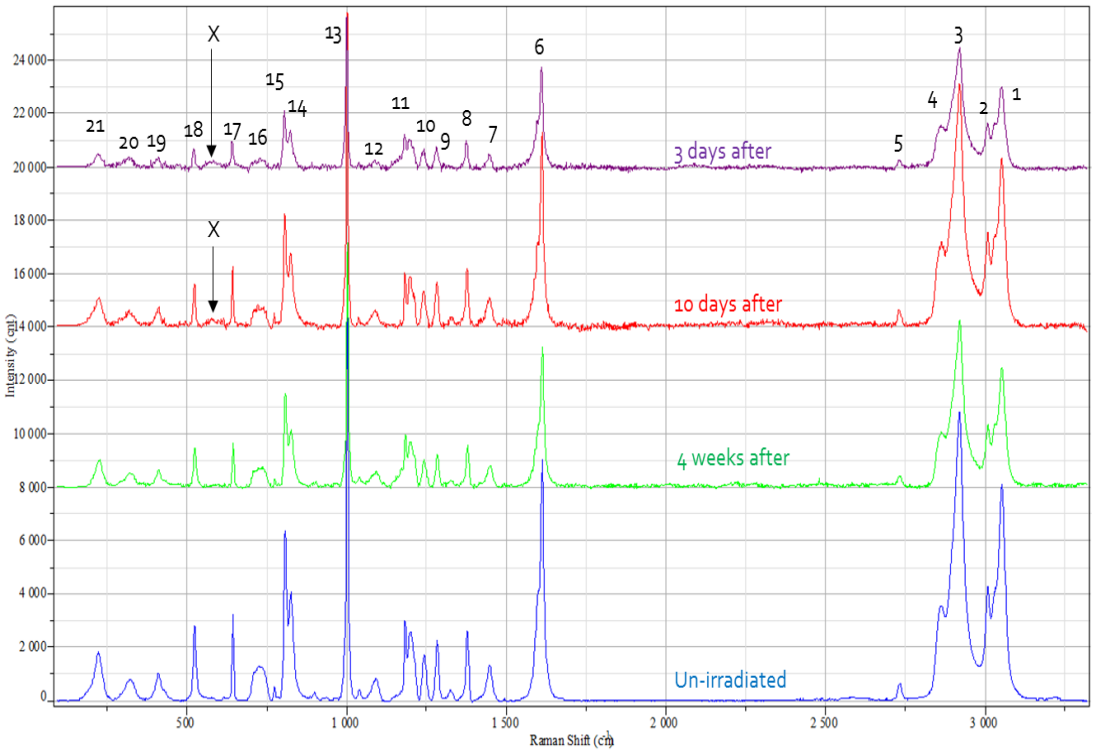

Figure 3: Background subtracted Raman spectra for 8 MGy irradiated EJ200.
N.B Spectra overlap but intensities have been shifted in order to have better visible representation.

Table 2: Allocation of peaks to characteristic functional groups or vibrational groups.

Functional Group/ Vibration	Peak Assignment
δ(C-C) aliphatic	20-21
ν(C-C) alicyclic or aliphatic chain vibrations	9-12, 14-19, X
ν(C-C) aromatic ring chain vibrations	13
δ(CH3)	8
δ(CH2) or δ(CH3)asymmetric	7
ν(C=C)	6
ν(C-H)	3-4
ν(=(C-H))	1-2

The ratio of species typically found in the vinyl backbone of the sample versus that in the benzene ring shows an increase after irradiation. A small amount of additional alicyclic rings and aliphatic chains are found with the additional peak X being typical of these bonds. These bonds represent single carbon rings and chains stripped of hydrogen. This indicates that structural damage occurs within the scintillator whereby bonds in the benzene ring are broken. Hydrogen may be lost by the benzene rings to form free radicals. After 4 weeks of healing, the scintillator appears to substantially recover its structure.

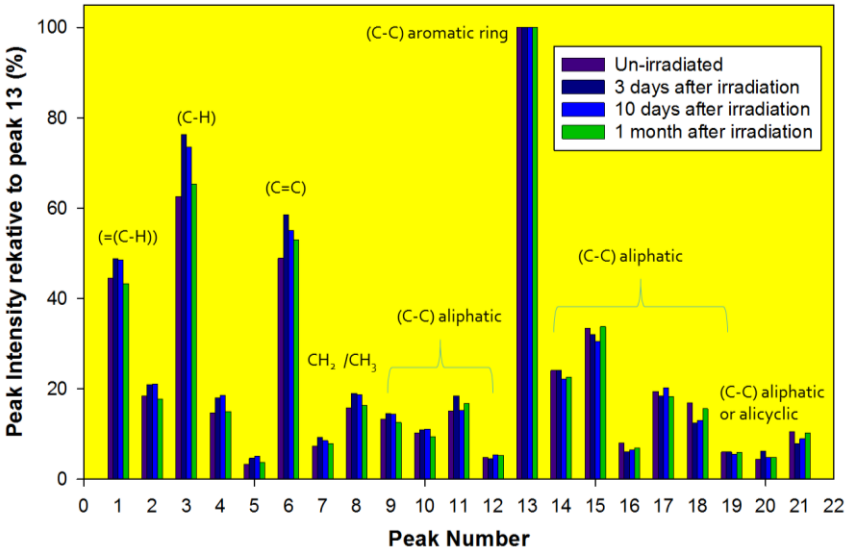

Figure 4: Plot of the intensities of peaks relative to peak 13 representing the C-C aromatic ring bond.

6. Conclusion

According to the results obtained in this study, irradiation to high doses in plastic scintillator EJ200 using 6 MeV protons causes radiation damage and leads to a reduced performance in its scintillation capabilities. At a dose of approximately 0.8 MGy, the structure of the scintillator remains robust, however scintillation light loss may still occur since light transmission results indicate that a competitive absorptive process develops between the primary and secondary fluors.

At a dose of 8 MGy, the scintillator becomes less transparent to its own light. The formation of an absorptive tint indicates that free radicals may be absorbing light that would otherwise be collected from the scintillator. These free radicals may arise from hydrogen that is lost through bonds breaking within the benzene rings of the polyvinyl toluene base and hence leading to additional aliphatic chains and alicyclic rings observed in the Raman spectra. The Raman spectra further indicate that after 4 weeks, the scintillator significantly recovers its structure. As the irradiation dose is increased, a greater loss to light transparency is observed. This can also be visibly noticed in the increased yellowing of the irradiation spot among samples with progressing higher doses. Increasing dose leads to greater structural damage and which in turn will lead to a greater reduction in the light output of the scintillator.

Overall, EJ200 can be considered as substantially radiation hard since for a dose of 0.8 MGy, it still maintains its structural composition and remains fairly transparent. It is only at doses higher than 8 MGy that permanent structural damage occurs. The highest dose currently expected within the Tile Calorimeter over the next several years is 10 kGy and therefore EJ200 may be a potential candidate for consideration during the 2018 replacement of the GAP scintillators. Light yield studies will need to be taken into account however, before this conclusion can be confirmed.

7. Upcoming work

This study is being carried out on several other plastic scintillators including PVT based EJ208, EJ260 and BC-408 obtained from ELJEN technologies and Saint Gobain Crystals respectively. These commercial scintillators will be compared to the polystyrene based scintillators presently used within the Tile Calorimeter. In addition to the techniques looked at in this paper, healing in the scintillators as well as the effect of dose rate on the damage induced are being looked at. Electron Paramagnetic resonance (EPR) and nuclear magnetic resonance (NMR) studies are also being conducted in order identify the types of free radicals formed due to radiation damage.

References

[1] ATLAS Collaboration, “The ATLAS Experiment at the CERN Large Hadron Collider,” IOP Publishing and SISSA, 2008.

[2] G. F. Knoll, “Chapter 8: Organic Scintillators,” in *Radiation Detection and Measurement, Third Edition*, Michigan, John Wiley & Sons, Inc., 1999, pp. 220-222.

[3] M. Chen, “Queen's University, PHYS 352: Measurement, Instrumentation and Experiment Design,” 4 May 2011. [Online]. Available: http://www.physics.queensu.ca/~phys352/lect19.pdf

[4] Universität Heidelberg, “Scintillation Detectors: Particle Detection via Luminescence,” 8 May 2011. [Online]. Available: http://www.kip.uni-heidelberg.de/~coulon/Lectures/Detectors/Free_PDFs/Lecture4.pdf

[5] ELJEN Technology, “Products: Plastic Scintilators,” [Online]. Available: http://www.eljentechnology.com/index.php/products/plastic-scintillators. [Accessed 12 October 2013].

[6] C. Zorn, “A PEDESTRIAN’S GUIDE TO RADIATION DAMAGE IN PLASTIC SCINTILLATORS,” *Radiat. Phys. Chem.,* vol. 41, no. 1/2, pp. 37-43, 1993.